SolarPACES 2023, 29th International Conference on Concentrating Solar Power, Thermal, and Chemical Energy Systems

Solar Collector Systems

https://doi.org/10.52825/solarpaces.v2i.953

Published: 24 Jul. 2024

Performance of a Prototype Heliostat Having a Twisting Mechanism to Maintain Focus Throughout the Day

Roger Angel[1,2], Nick Didato[1], Matt Rademacher[1], and Yiyang Huang[2]

[1] Steward Observatory, University of Arizona, USA

[2] Wyant College of Optical Sciences, University of Arizona, USA

Abstract. A prototype heliostat has been designed and built with a rectangular reflector whose shape is altered automatically through the day, to maximize concentration at the receiver. The shape changes needed to form solar disc images, which give the highest possible concentration, can be realized by twisting the reflector from its corners, provided that a target-oriented, dual-axis mount is used. Then a cam mechanism connected to the second (cross) axis drive, turning with the angle of incident sunlight, may be used to twist the reflector as needed. Our prototype reflector comprises a single glass mirror, 2.4 m x 3.3 m, attached to a steel frame. Four diagonal back struts extend from the central mechanism out to the rectangular frame corners. The glass mirror of the prototype is attached to the steel frame by 58 screw actuators. Before twisting the frame, the glass shape is adjusted to the biconic shape needed to form a 1 m diameter disc image on a 113 m distant target when sunlight is incident at 60°. To form disc images over the full range of angles of incidence from 0° (normal incidence) to 70°, the struts push the corners up and down by up to 17 mm. A reflectometry metrology system has been used to set the 58 adjustment screws for the initial shape to an accuracy of ≤ 0.6 mrad, and to measure the accuracy of the different twisted shapes. The prototype will be tested at NSTTF early next year.

Keywords: Heliostat, Twisting Reflector, High Concentration

1. Introduction

To increase the efficiency of generating electricity, and to increase thermal processing capabilities, heliostat receivers need to achieve temperatures beyond what is currently achievable, and thus higher concentrations of sunlight are required. One way that has been employed to achieve high concentration is to use flat heliostats to direct sunlight onto a large static concave paraboloidal reflector to focus sunlight onto the receiver target. Various CSP, CPV, and telescope systems use this method for research. But for commercially viable heliostat fields, focusing directly to a receiver, the angle of incidence (AOI) on any reflector changes as the sun moves across the sky throughout the day. To maintain a focus on the receiver under these circumstances, the reflector shape must also change throughout the day. The shapes required for focusing sunlight striking at different AOIs are different concave biconics, whose two principal radii of curvature in the tangential and sagittal directions are functions of the AOI. Furthermore, the tangential biconic must be held in the plane of incidence. The two biconic radii of curvature, in the tangential plane (R_T) and sagittal plane (R_S), are given by:

$$R_T = R/\cos(AOI) \tag{1}$$

$$R_S = R\cos(AOI) \quad (2)$$

Where R is twice the distance between the heliostat and the receiver (i.e., focal distance).

One concept for an actively shaped heliostat was demonstrated by Angel et al. [1]. A hexagonal reflector was used on an alt-az mount, and the two biconic radii were adjusted using 3 pairs of actuators pushing or pulling on the 6 corners of the reflector frame. A disadvantage of using an alt-az mount is that the orientation of the plane of reflection is constantly changing with respect to the reflector, as well as the two biconic radii of curvature, and shape adjustment requires computer control of three degrees of freedom.

A more recent concept described by Didato et al. [2] employs a rectangular reflector on a target-axis mounted system, with the advantage that mechanical coupling suffices to control its shape through the day. This is made possible because the target axis of the dual axis mount points directly to the receiver, and thus lies in the plane of incidence. To move the image of the sun onto the target, the target axis is rotated until the second axis, denoted as the "cross-axis", which is perpendicular to the target axis, is set also perpendicular to the plane of incidence. Rotation of the cross axis is then used to set the correct AOI to reflect the sunlight to the target. In this way, the plane of incidence is fixed in orientation with respect to the heliostat reflector. Figure 1 shows the shape of the glass rectangle with the two principal curvatures at 45 degrees to the rectangle edges. The desired different biconic shapes may be adjusted simply by twisting the glass from its 4 corners and center. The reflector is attached to the cross-axis drive at 45°, so that the tangential axis is oriented parallel to the cross axis, and the required biconic shapes may be attained using a mechanical linkage with two mechanical cam couplings to the cross-axis drive.

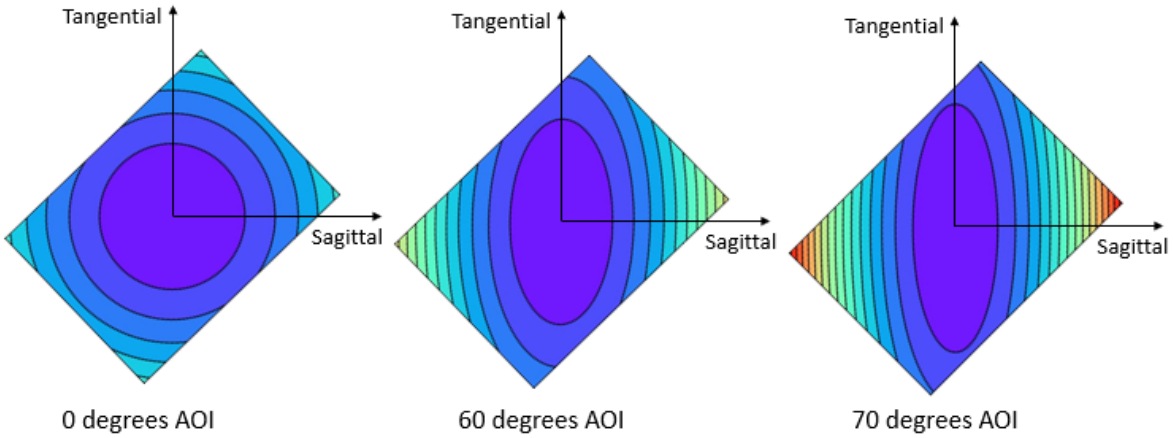

Figure 1. *Contours for the biconic shapes for 0, 60, and 70° AOI*

Didato et al. studied a design concept in which the reflector is a single 96 x 130 in. (2.44 m x 3.30 m) rectangular sheet of 1/8 in. (3.2 mm) thick, silvered float glass mounted to a flat steel frame. The glass is attached to the steel frame on 58 pads with a silicone adhesive. Attached to the rear side of the frame is a central mast which connects the frame to the post, along with two pairs of back struts which connect the corners of the frame to the shape-changing mechanism on the cross-axis drive. The frame layout is shown in Figure 2.

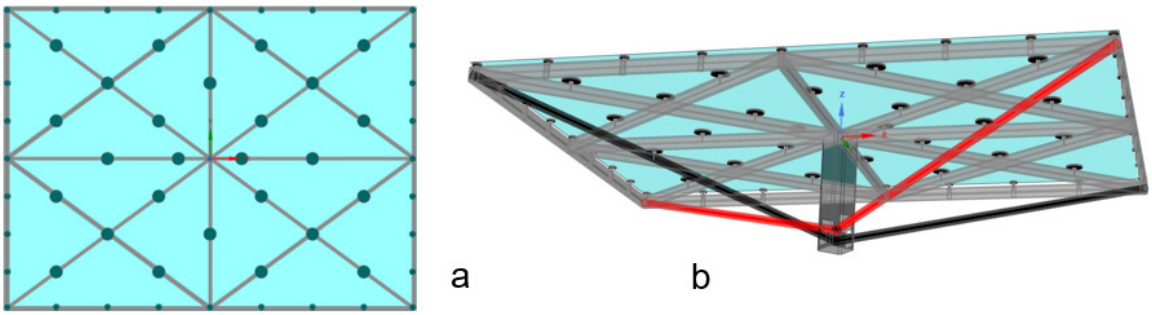

Figure 2. *Heliostat reflector frame design top-down (a) and side view showing the back struts and central mast (b).*

Since the biconic is symmetrical about the origin, the displacement of opposite corners will be equal for every required shape, thus they can be actuated in pairs as shown in Figure 2. To reduce the amount of force required to bend the frame into the proper shape, the 58 pads are initially adjusted in height to induce a "neutral toroid", which is in the middle of the corner-corner sag range from 0° AOI to 70° AOI. This neutral shape was determined to be the required toroid at 60° AOI.

2. Construction of an 8 m^2 twisting heliostat

2.1 Reflector Frame and Twisting Struts

Figure 3a shows a front view of the first prototype twisting reflector that has now been built. It will shortly be installed on a portable target-oriented mount shown in the SolidWorks rendition of Figure 3b. Visible in the center of the reflector is a spot where the back silvering of the glass has been removed. A fisheye camera for closed loop tracking will be mounted behind this spot.

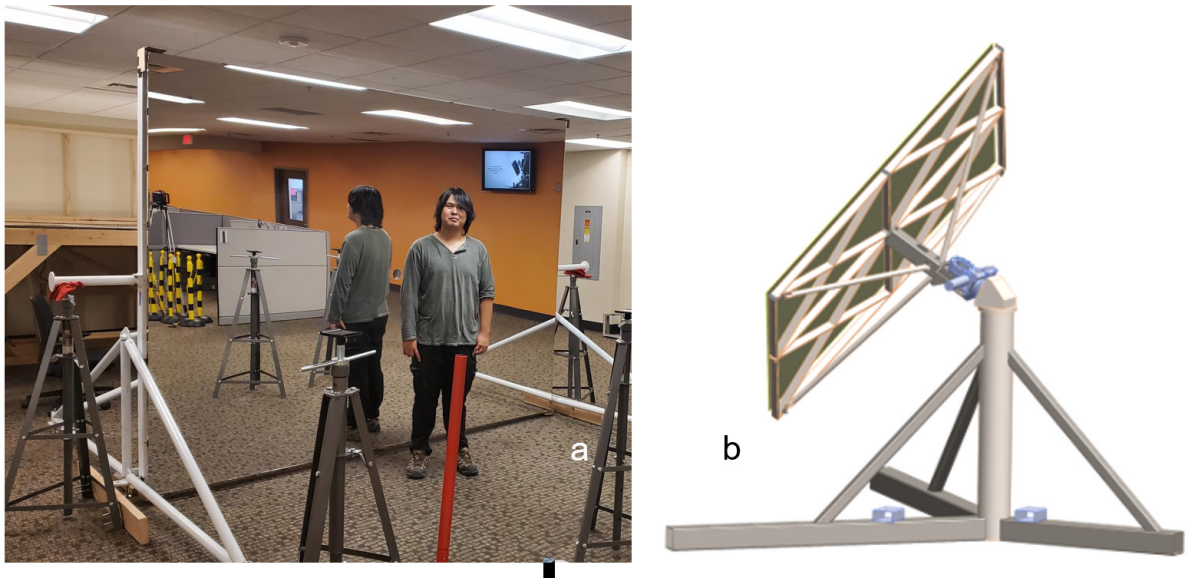

Figure 3. *(a) Prototype reflector (b) Rendition of portable target-oriented mount*

Figure 3. *Back view of the reflector*

Figure 4 shows a back view of the reflector, with the frame and central back strut in white and the four twisting struts to the corners in yellow. The struts are connected in diagonal pairs to two central clevises whose axial motion twists the frame. The screw knobs used to adjust the heights of the 58 attachment points to set the glass shape relative to the frame are visible, most clearly along the left vertical edge of the frame.

In this initial configuration for calibration of the twisting, the motion of the yellow strut pairs is made using temporary linear actuators to drive the axial stroke of the two central clevises. To measure the twisting for given clevis motion, two thin fishing lines were stretched from corner to corner across the mirror diagonals, and the sagittal depth at the center was measured. Figure 5 shows the twisting action, with the sagittal depth change almost one-to-one with clevis motion, as expected. There is very little hysteresis.

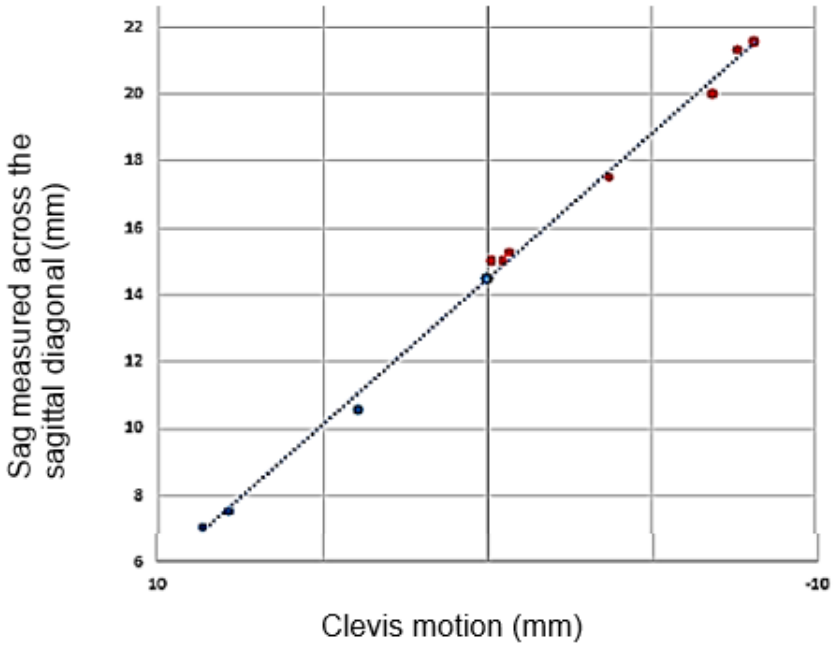

Figure 4. *Sag measured across the reflector diagonal vs clevis motion*

2.2 Cam twisting mechanism

The mechanism that couples the dual axis slew bearings to the diagonal struts is shown in a cut-away schematic in Figure 6(a). The cam plate, shown also in Fig 6(c), is rigidly attached to the mechanism base plate turned by the target axis drive. The cross-axis drive (8) turns the reflector frame via the angle plate 60 and the center strut 7. Rotation of the cross axis turns bearings 65 around the cam slots, which are coupled to and move up and down the clevises

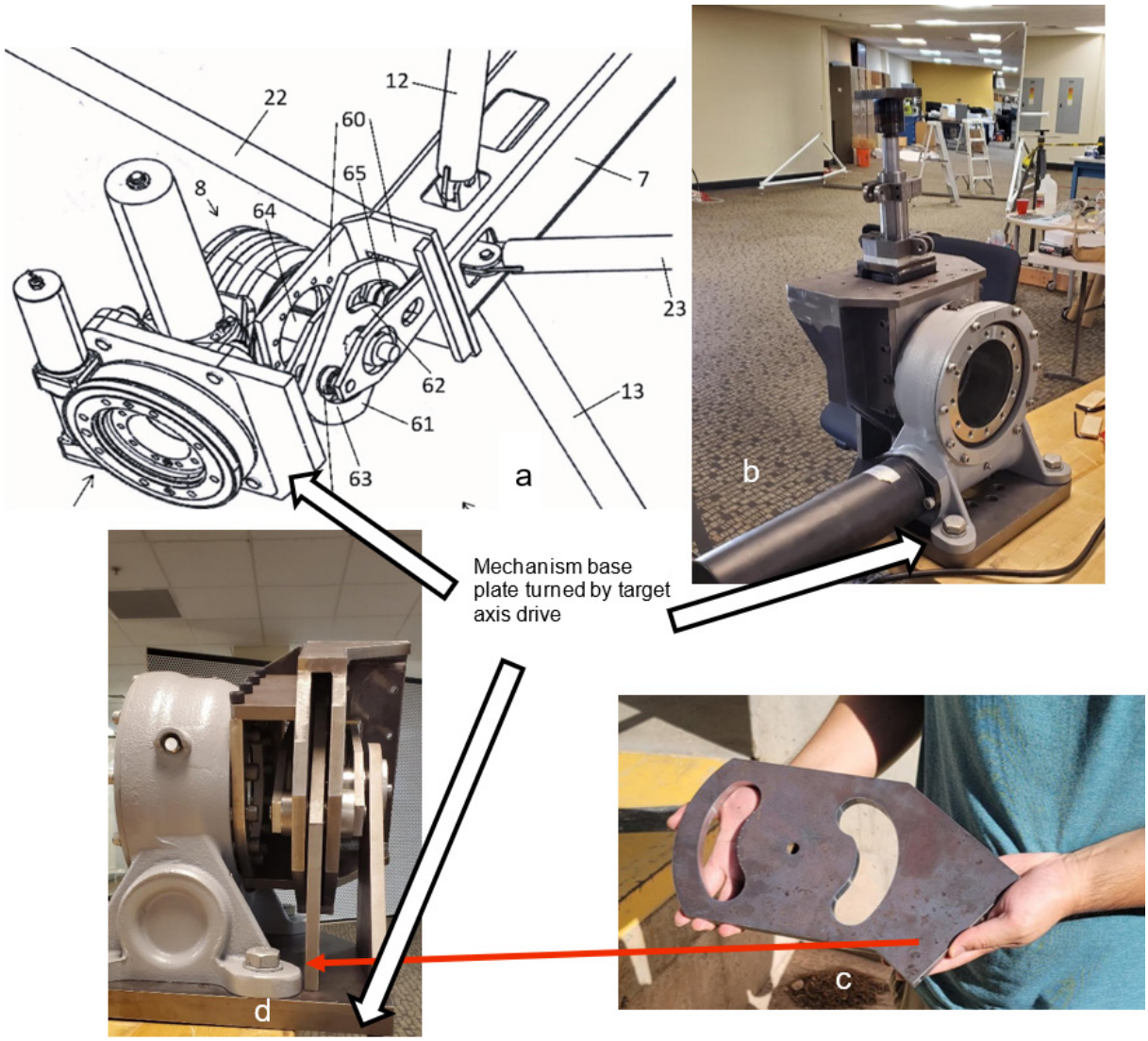

Figure 6. *(a) Cutaway schematic of the dual axis slew bearings and cam mechanism (b) cross-axis rive with mechanism set for 0° AOI and the two clevises driven in the vertical direction (c) cam plate before assembly (d) side view with the mechanism et for 70° AOI*

and the diagonal strut pairs 12 and 13 and 22 and 23. Figure 6(b) shows the cross-axis drive with mechanism set for 0° AOI and the two clevises driven in the vertical direction. Figure 6(d) shows a side view with the mechanism set for 70° AOI. Bearing in mind that in high wind, force on the reflector will be taken in part by the mechanism, it is made from ½" thick steel. With bearings designed to take 1000 lb. loads.

To measure the accuracy of action of the cam mechanism, dial indicators were attached to measure the motions of the two clevises as a function of rotation of the cross-axis drive. Figure 7 below shows the measured positions as blue(sagittal) and red (tangential) spots, and the motions needed to obtain the targeted biconic radii of equations 1 and 2 above shown as

dotted lines. The accuracy motions are accurate to < 1 mm, which corresponds to a largest slope error (at the reflector corners) of < 0.5 mrad.

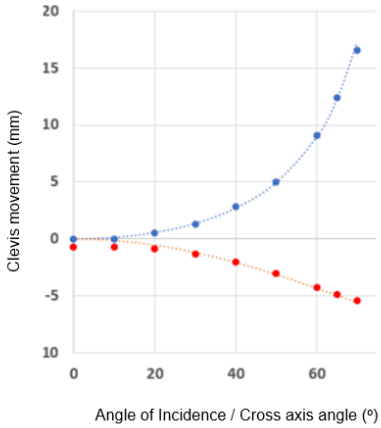

Figure 7. *Clevis motion measured as a function of rotation of the cross-axis drive*

3. Measured surface shape and slope errors

Measurements of the reflector surface have been made by high-resolution reflectometry. In this method, slope errors in the reflector surface show up as distortion in the reflection seen in the heliostat mirror of a screen with a regular grid of white spots. A plan view of the optical configuration used in the lab is shown in Figure 8 below. A spatial resolution of 25 mm is obtained by using spots in a grid with this spacing. With the screen 12.5 m from the reflector, a slope error at the reflector of 1 mrad shows as a screen spot displacement of 25 mm. In practice, accuracy of 0.1 mrad rms is achieved. Further details of the method are given by Kim et al., [3].

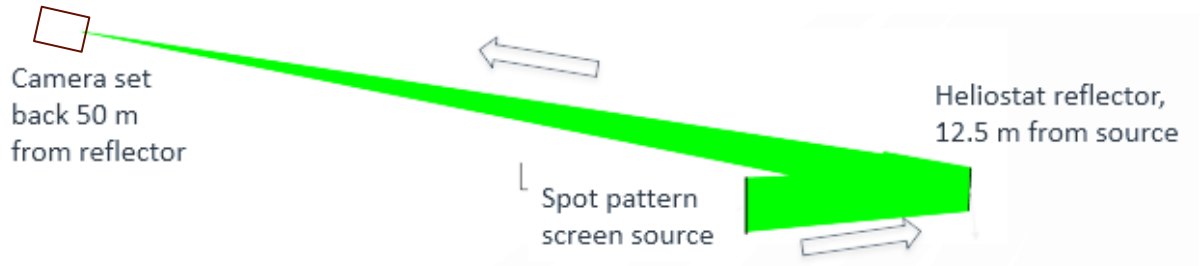

Figure 8. *Plan view of the reflectometry metrology configuration*

Figure 9 shows the results of metrology of the reflector set with no frame bending, targeting the shape needed for sunlight incident at 60° angle of incidence. The elliptical contours of the desired shape are shown in Figure 9a, while the measured actual reflector shape is shown in Figure 9b. Contours of the difference in the two shapes are shown in Figure 9c, the error map. The error is 0.12 mm rms.

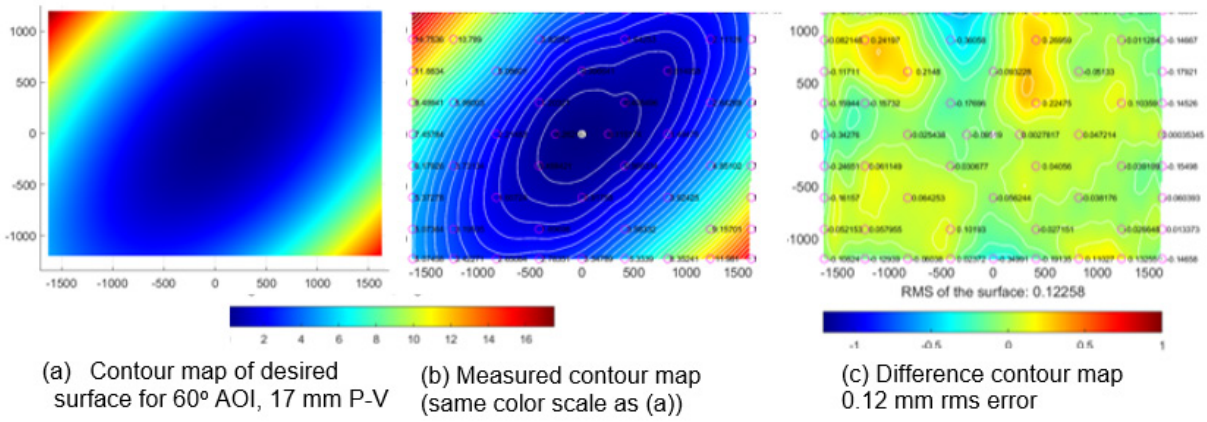

Figure 9. *Measurements of the reflector set for 60° angle of incidence*

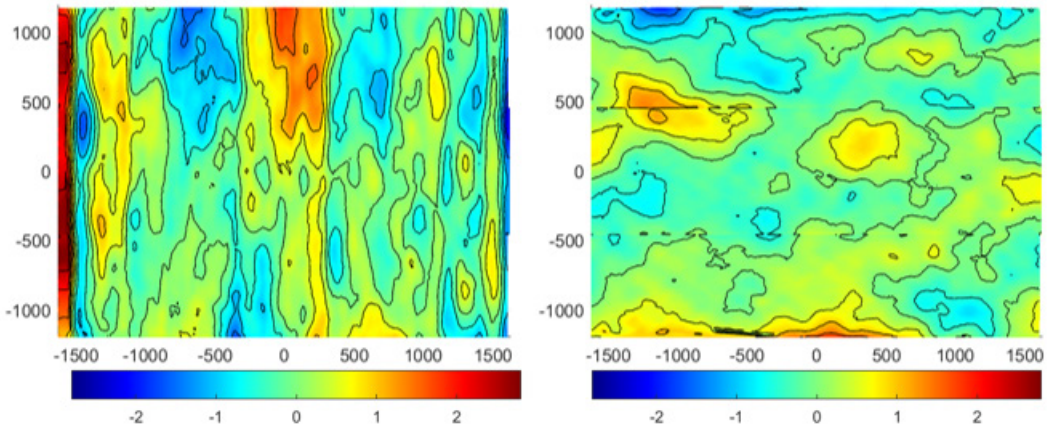

Figure 10. *Slope errors from the error contour map, Figure 9(c)*

The reflector surface slope errors derived from the error contour map Figure 9(c) are shown in Figure 10. The average rms errors are 0.66 mrad in the x direction and 0.41 mrad in the y direction. The x-slope errors are larger because of vertical ripples in the float glass of rms amplitude 0.5 mrad. The wavelength of these ripples is ~ 30 cm, too small to be correctable by adjustment of the 58 screw actuators.

4. Discussion

We are now ready to take the step of mounting the reflector, cam mechanism and target-axis drives on the pedestal illustrated in Figure 3(b) and obtain images of the solar disc through the day, at different angles of incidence. These tests are to be made at the U. Arizona Tech Park, and in the new year with Randy Brost at the NSTTF. In the meantime, from ray trace modeling using metrology data, we have already a good idea of what to expect.

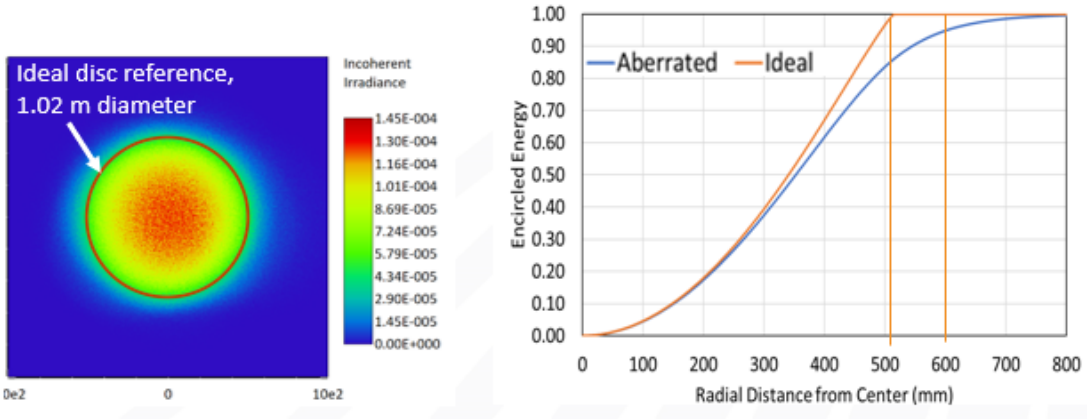

Figure 11. *Disc image of the sun calculated by ray tracing for the measured reflector.*

Figure 11 shows the disc image calculated by ray tracing for the reflector surface with the errors shown in Figures 9 and 10. A perfect image at the 113 m receiver distance would be 1.02 m in diameter, while the calculated aberrated image places 95% within a circular aperture of 1.2 m diameter, i.e. a geometric concentration of 7.1 for the single heliostat.

In practice additional errors from errors in the twisting and heliostat orientation will further reduce the 1.2 m diameter encircled energy, as will blocking, shadowing, and cosine loss. However, even with these additional losses, high concentration over much of the day will be achievable. In a model [2], with 450 heliostats powering five compound paraboloidal concentrators, a concentration of > 3,000 was obtained at powers > 1 MW, through much of the day.

Data availability statement

The data that support the findings of this study are available from the corresponding author, [R.A.] upon reasonable request.

Author contributions

Angel: conceptualization, methodology, writing and supervision, investigation, funding acquisition; Didato: methodology, software, formal analysis, writing, visualization; Rademacher: methodology, validation, investigation, resources, supervision; Huang: methodology, formal analysis, investigation, data curation, visualization.

Competing interests

The authors declare that they have no competing interests.

Funding

This work is supported by the DOE through EERE - SETO, and NREL - Heliocon

References

[1] R. Angel, R. Eads, N. Didato, N. Emerson, C. Davila, “Actively Shaped Focusing Heliostat,” AIP Conference Proceedings 2445**,** 2022
[2] N. Didato, R. Angel, M. Rademacher, “Shape-adjustable heliostats: designs for individuals and fields for > 3000 concentration,” SPIE, 2023 http://dx.doi.org/10.1117/12.2681483.
[3] Kim, Y. Huang, H. Tailor, R. Su, H. Kang, H. Choi, and R. Angel, “Static Screen Deflectometry for Twisting Heliostat Mirrors”, SolarPACES 2023, 2023